Published in final edited form as:
J Cell Sci. 2007 December 1; 120(Pt 23): 4134–4143. doi:10.1242/jcs.015834.

The increase of cell-membranous phosphatidylcholines containing polyunsaturated fatty acid residues induces phosphorylation of p53 through activation of ATR

Xu Hannah Zhang, **Chunying Zhao**, and **Zhongmin Alex Ma***
Division of Experimental Diabetes and Aging, Department of Geriatrics and Adult Development, Mount Sinai School of Medicine, New York, NY 10029, USA

Summary

The G1 phase of the cell cycle is marked by the rapid turnover of phospholipids. This turnover is regulated by CTP:phosphocholine-cytidylyltransferase (CCT) and group VIA Ca^{2+}-independent-phospholipase A_2 ($iPLA_2$). We previously reported that inhibition of $iPLA_2$ arrests cells in G1 phase of the cell cycle by activating the p53-p21 checkpoint. Here we further characterize the mechanism of p53 activation. We show that specific inhibition of $iPLA_2$ induces a time dependent phosphorylation of Ser15 in p53 in the absence of DNA damage. This phosphorylation requires the kinase ataxia-telangiectasia and Rad-3-related (ATR) but not the ataxia-telangiectasia-mutated (ATM) kinase. Moreover, we identify in cell membranes a significant increase of phosphatidylcholines (PCs) containing chains of polyunsaturated fatty acids and a decrease of PCs containing saturated fatty acids in response to inhibition of $iPLA_2$. The time course of phosphorylation of Ser15 in p53 correlates with increasing levels of PCs containing polyunsaturated fatty acids. We further demonstrate that the PCs with linoleic acid in their sn-2 position (18:2n6) induce phosphorylation of Ser15 in p53 in an ATR-dependent manner. Our findings establish that cells can regulate the levels of polyunsaturated fatty acids in phospholipids through $iPLA_2$-mediated deacylation of PCs. Disruption of this regulation increases the proportions of PCs containing polyunsaturated fatty acids and activates the ATR-p53 signalling pathway.

Keywords

Group VIA Ca^{2+}-independent phospholipase A_2 ($iPLA_2$); Phospholipid turnover; Phosphatidylcholine; Polyunsaturated fatty acids; Phosphorylation of p53; Ataxia-telangiectasia-mutated (ATM) kinase; Ataxia-telangiectasia and Rad-3-related (ATR) kinase

Introduction

Cellular membranes in mammalian cells are dynamic and fluid structures that undergo dramatic structural and functional changes during the cell cycle, including the complete breakdown and reformation of the nuclear envelope and the fragmentation and stack reformation of the Golgi membrane (Burke and Ellenberg, 2002; Colanzi et al., 2003). Phosphatidylcholines (PCs) are a main component of cellular membrane phospholipids and their metabolism varies throughout the cell cycle (Jackowski, 1996; Lykidis and Jackowski,

*Author for correspondence (zhongmin.ma@mssm.edu).

Supplementary material available online at http://jcs.biologists.org/cgi/content/full/120/23/4134/DC1

2001). Cells in G1 rapidly synthesize and degrade PCs, while still maintaining a constant total membrane phospholipid mass (Jackowski, 1994). By contrast, PC turnover ceases in S phase to allow the cells to double their membrane-phospholipid content in preparation for cell division. Finally, even though cellular membranes are undergoing dramatic structural changes in G2 and M, the synthesis and degradation of membrane phospholipid components are at their lowest at this point in the cell cycle (Jackowski, 1994; Jackowski, 1996).

Although it is not clear why mammalian cells experience such a rapid phospholipid turnover during G1, it has become evident that this process is regulated through the coordination of the opposing actions of CTP:phosphocholine cytidylyltransferase (CCT) and the group VIA Ca^{2+}-independent-phospholipase A_2 ($iPLA_2$, also known as $iPLA_2\beta$) (Baburina and Jackowski, 1999; Barbour et al., 1999). $iPLA_2$ hydrolyzes the sn-2 fatty-acyl bond of phospholipids to liberate free fatty acids and lysophospholipids (Ma and Turk, 2001). Because the sn-2 of phospholipids are preferentially linked to polyunsaturated fatty acids, it is possible that this reaction is important to regulate the ratio of saturated to unsaturated hydrocarbon chains in the phospholipids and to control the fluidity of cellular membranes.

We previously found that inhibiting $iPLA_2$ disrupts this phospholipid turnover and induces a p53-dependent cell-cycle arrest in G1 (Zhang et al., 2006). Our finding suggests that, not only is G1 phospholipid turnover a programmed cellular event required for S-phase entry but also the progress of this turnover is monitored by a p53-dependent checkpoint. Activation of p53 to prevent cells from inappropriately entering the S phase of the cell cycle may be one way cellular membranes regulate DNA replication.

The p53 pathway coordinates DNA repair, cell-cycle arrest, apoptosis and senescence to preserve genomic stability and prevent tumor formation in response to cellular insults (Campisi, 2005; Vogelstein et al., 2000). p53 levels are tightly controlled in unstressed mammalian cells through a continuous cycle of ubiquitylation and degradation by the 26S proteasome, regulated primarily through the interaction of p53 with the ring-finger ubiquitin E3 ligase MDM2 (Yang et al., 2004). Whereas most studies on p53 have focused on its role in preserving genomic stability (Bode and Dong, 2004), recent work suggests that p53 might also be important for the glucose-availability cell cycle checkpoint (Jones et al., 2005), for energy control and metabolism (Bensaad et al., 2006; Matoba et al., 2006) and for G1 phospholipid homeostasis (Zhang et al., 2006).

Post-translational modifications of p53, including phosphorylation and acetylation, are common ways to activate p53 in response to DNA damage (Bode and Dong, 2004; Gu et al., 2004). In this study we investigate how p53 is activated in response to the perturbation of phospholipid homeostasis. We used lipidomic analysis to determine whether and how phospholipid profiles change after $iPLA_2$ inhibition. We found that $iPLA_2$ inhibition induces the phosphorylation of p53 at Ser15 (hereafter referred to as p53S15) in an ATR-dependent manner. Furthermore, we identified a significant increase in PCs containing polyunsaturated fatty acids and a decrease in PCs containing saturated fatty acids in cell membranes following $iPLA_2$ inhibition. We propose that $iPLA_2$ regulates cell membrane fluidity by controlling the levels of polyunsaturated fatty acids in PCs and that an increase of the ratio of polyunsaturated to saturated fatty acids in PCs activates ATR.

Results

Inhibition of $iPLA_2$ induces the rapid phosphorylation of p53 at Ser15

We have recently reported that inhibiting $iPLA_2$ activates the p53-p21 pathway and arrests the cell cycle in G1 (Zhang et al., 2006). To gain further insight into the mechanism of p53 activation, we investigated whether inhibition of $iPLA_2$ induces phosphorylation of p53 at

Ser15, a phosphorylation that commonly occurs in response to DNA damage (Bode and Dong, 2004). As shown in Fig. 1A, inhibition of $iPLA_2$ by the $iPLA_2$-specific inhibitor bromoenol lactone (BEL) induced both the phosphorylation of p53 at Ser15 and the accumulation of p53 protein in a concentration-dependent fashion. To confirm that this p53 phosphorylation is specifically caused by $iPLA_2$ inhibition, we silenced the expression of $iPLA_2$ with $iPLA_2$-specific siRNA. As shown in Fig. 1B, silencing of $iPLA_2$ in HCT116 cells also induced phosphorylation of p53 at Ser15.

We further examined the time course of BEL-induced phosphorylation of p53 at Ser15. Not only were we able to detect p53S15 phosphorylation after 30 minutes of BEL treatment, this phosphorylation continued to increase with time. This increase was accompanied by a corresponding rise in the total amount of p53 protein (Fig. 1C,D). Both p21 and MDM2 are transcriptional targets of p53 (Barak et al., 1993). As shown in Fig. 1D, MDM2 accumulates in response to p53S15 phosphorylation. These results suggest that, although other post-translational modifications might also be involved, phosphorylation of p53 at Ser15 activates p53 and causes it to accumulate in response to inhibition of $iPLA_2$.

To test whether this pathway exists in primary cells, we treated human primary foreskin fibroblasts with 10 or 15 μM BEL for 10 hours and assessed the phosphorylation status of p53. As shown in Fig. 1E, inhibition of $iPLA_2$ by BEL also induced phosphorylation of p53 at Ser15 in human primary cells, confirming the biological significance of this pathway.

Inhibition of $iPLA_2$ by BEL does not induce DNA damage

Most reports on Ser15 phosphorylation of p53 are focused on the effects of DNA-damage inducers. To evaluate whether $iPLA_2$-inhibition causes similar DNA damage, we used western blotting to measure the phosphorylation of histone H2AX at Ser139, a marker for DNA breaks (Fernandez-Capetillo et al., 2004; Rogakou et al., 1998). As shown in Fig. 2A, treatment of HCT116 cells with BEL for 8 hours induced phosphorylation of p53 at Ser15 in a concentration-dependent fashion. This phosphorylation correlated with the enhanced induction and functional activation of p53 as measured by increasing amounts of transcription of the p53 target p21 (CDKN1A). However, we did not detect any phosphorylation of H2AX at Ser139 in HCT116-$p53^{+/+}$ cells, even after 28 hours of treatment with 12.5 μM BEL (Fig. 2A). By contrast, doxorubicin (Dox), a DNA-damaging agent known to activate p53 through phosphorylation of Ser15 (Kurz et al., 2004), dramatically increased levels of both phosphorylated p53 and H2AX (p53-*P* and H2AX-*P*, respectively) (Fig. 2A).

We have previously shown that G1 arrest in response to $iPLA_2$ inhibition requires both p53 and p21. Cells without p21 become apoptotic (Zhang et al., 2006). Because it has also been demonstrated that the initiation of DNA fragmentation during apoptosis induces the phosphorylation of histone H2AX at Ser139 (Rogakou et al., 2000), we reasoned that this phosphorylation should be observed in HCT116 cells that do not express p21 (HCT116-$p21^{-/-}$ cells) treated with BEL and undergoing apoptosis. To test this, we incubated HCT116-$p21^{-/-}$ cells with increasing concentrations of BEL and analyzed the phosphorylation of H2AX at Ser139. As predicted, we found that levels of H2AX-*P* in HCT116-$p21^{-/-}$ were dependent on the concentration of BEL and that, consistent with a previous report (Rogakou et al., 2000), this phosphorylation can be blocked by caspase inhibitor (Fig. 2B). These results strengthen our contention that BEL treatment itself does not cause double-stranded (ds) DNA breaks in HCT116 cells.

We next confirmed the results of our western blot analysis by examining H2AX phosphorylation in situ with the more sensitive methods of immunofluorescence and confocal fluorescence microscopy. As shown in Fig. 2C (in a population of cells) and Fig.

2D (in a single nucleus), DNA damage induced by a low dose of doxorubicin can easily be detected by immunofluorescence staining of H2AX-*P*. By contrast, treatment of cells with 12.5 μM BEL for up to 8 hours did not induce the phosphorylation of H2AX at Ser139. To confirm that immunofluorescence staining of H2AX-*P* is sensitive enough to detect even small amounts of dsDNA damage, we treated the cells with a low dose of doxorubicin (0.2 μg/ml) for 2 and 8 hours. We found that dsDNA damage can be detected after only 2 hours of doxorubicin treatment even though phosphorylation of p53 at Ser15 appears unchanged during this time (see Fig. S1 in supplementary material). Taken together, we concluded that Ser15 phosphorylation of p53 in response to $iPLA_2$ inhibition is unlikely to be due to dsDNA damage in HCT116-$p53^{+/+}$ cells.

We next used TUNEL assay to detect the free 3′-OH termini of DNA breaks that might be caused by inhibition of $iPLA_2$. As shown in Fig. 2E, in contrast to cells treated with UV light, cells treated with 10 μM or 15 μM BEL for 8 hours exhibited little TUNEL staining. We then titrated the UV dose to ensure that TUNEL staining is sensitive enough to detect the levels of single-stranded (ss) DNA damage at which Ser15 phosphorylation of p53 is apparent. We found that 10 J/m^2 UV induces levels of ssDNA damage detectable by TUNEL even though levels of p53-*P* appear unchanged (see Fig. S2 in supplementary material).

Finally, we confirmed the above results in individual cells through the alkaline version of the comet assay, which can detect a variety of DNA damage including single-strand breaks, double-strand breaks, alkali-labile sites, incomplete excision-repair sites and DNA crosslinks (Olive and Banath, 2006). As shown in Fig. 2F, although UV light caused the ‘comet’ migration pattern characteristic of relaxed DNA, BEL treatment resulted in neither the relaxation of nuclear DNA (sharp edge) nor the comet pattern. Quantitative analysis of comet assay results showed that the tail moments of BEL-treated cells were no different from those of the controls but significantly different from those of UV light treatment. Taken together, our data demonstrate that the phosphorylation of p53 at Ser15 induced by $iPLA_2$ inhibition is independent from any type of DNA damage detectable by current methods.

BEL-induced phosphorylation of p53 at Ser15 is caffeine sensitive

BEL-induced p53-*P* can be detected after only 30 minutes of BEL treatment (Fig. 1C). Such rapid phosphorylation suggests the activation of upstream p53 kinases such as ataxiatelangiectasia-mutated (ATM) kinase, or ataxia-telangiectasiaor Rad-3-related- (ATR) kinase (Banin et al., 1998;Canman et al., 1998;Tibbetts et al., 1999). We therefore examined levels of p53-*P* after BEL treatment in the presence of caffeine, which inhibits ATM and ATR kinase activities (Blasina et al., 1999;Sarkaria et al., 1999). As shown in Fig. 3, not only was BEL-induced p53-*P* reduced to near control levels by caffeine in both human HCT116 cells (Fig. 3A) and rat pancreatic β-cell line INS-1 cells (Fig. 3B), it was also accompanied by a significant reduction in the expression of p21. These findings suggest that perturbing G1 phospholipid homeostasis by inhibiting $iPLA_2$ in mammalian cells activates the ATM/ATRp53-p21 pathway. p21 then prevents CDK activation and arrests the cells in the G1 phase of the cell cycle (Massague, 2004;Zhang et al., 2006). Interestingly, cells treated with both caffeine and BEL exhibited higher levels of p53 and p21 than control cells (Fig. 3A), suggesting the existence of a p53 phosphorylation-independent pathway that stabilizes p53 in BEL-treated cells.

ATM is not required for phosphorylation of p53 at Ser15 in response to inhibition of $iPLA_2$

ATM and ATR kinases increase cell viability after genotoxic insult by phosphorylating p53 at Ser15 to initiate the G_1-S checkpoint (Canman et al., 1998; Delia et al., 2000; Tibbetts et

al., 1999). Because both kinases are inhibited by caffeine, it is not possible to determine from our previous result which of the two is activated through $iPLA_2$ inhibition. We therefore compared levels of p53-*P* in response to BEL treatment in ATM-deficient cells ($ATM^{-/-}$, GM01526 cells) with those in wild-type cells ($ATM^{+/+}$, GM01805 cells). As shown in Fig. 4A, treatment with BEL for 4 and 8 hours induced essentially the same levels of p53-*P* and total p53 protein in $ATM^{-/-}$ cells as in $ATM^{+/+}$ cells. This finding suggests that ATM does not play a major role in phosphorylation of p53 at Ser15 in response to perturbation of G1 phospholipid homeostasis.

We next investigated the effect of caffeine in $ATM^{-/-}$ cells treated with BEL. As shown in Fig. 4B, BEL-induced phosphorylation of p53 at Ser15 was blocked by caffeine in these cells. Interestingly, although BEL induced both the rapid phosphorylation of p53 at Ser15 and the accumulation of total p53 protein within 30 minutes, both of these responses were essentially blocked by pre-treating the cells with caffeine, indicating that early accumulation of p53 results mainly from phosphorylation of p53. However, the fact that p53 accumulates in $ATM^{-/-}$ cells after 3 hours of BEL treatment even in the presence of caffeine (which almost completely blocks p53S15 phosphorylation), suggests that other mechanisms involved in accumulation of p53. These results, together with the fact that we could not detect phosphorylation of H2AX at Ser139, suggest that ATM is not required for BEL-induced phosphorylation of p53 at Ser15.

ATR plays a major role in the phosphorylation of p53 at Ser15 in response to inhibition of $iPLA_2$ by BEL

Blocking BEL-induced phosphorylation of p53 at Ser15 by caffeine in $ATM^{-/-}$ cells suggests the involvement of ATR. To determine the role played by ATR in response to BEL, we used U2OS-derived osteosarcoma cells with doxycycline-inducible expression of either a dominant-negative form (kinase dead) of ATR (ATR-kd; U2OS GK41 cells) or wild-type ATR (ATR-wt; U2OS GW33 cells) (Nghiem et al., 2001; Nghiem et al., 2002) because ATR homozygous knockouts are lethal (Brown and Baltimore, 2000). Upon addition of doxycycline, these cells express FLAG-tagged ATR-wt or FLAG-tagged ATR-kd, which depletes native ATR activity.

Immunoblotting with anti-FLAG antibody confirmed the expression of the proteins after doxycycline treatment (Fig. 4C,D). We found that, although BEL-treated ATR-wt-expressing cells exhibited much higher levels of p53-*P* in the presence of doxycycline than in its absence, this phosphorylation can be significantly blocked by caffeine (Fig. 4C). By contrast, BEL induced significant phosphorylation of p53 at Ser15 in a concentration-dependent fashion in ATR-kd-expressing cells in the absence but not the presence of doxcycline (Fig. 4D). These results clearly show that, ATR is required for phosphorylation of p53 at Ser15 in response to inhibition of $iPLA_2$ and ATM can not compensate for lack of ATR function.

Inhibition of $iPLA_2$ results in an increase in PCs that contain polyunsaturated fatty acids

Membrane-phospholipid turnover in G1 is regulated through the coordinated biosynthesis of PC by CCT and its degradation by $iPLA_2$ (Baburina and Jackowski, 1999; Barbour et al., 1999; Jackowski, 1996). We speculated that inhibiting $iPLA_2$ may cause changes in a subset of phospholipids that affects cell cycle progression. To test this hypothesis, we cultured HCT116 cells with or without BEL for 24 hours, isolated the total phospholipids and profiled them with lipidomics. We found that inhibition of $iPLA_2$ by BEL caused a significant accumulation of PCs and a decrease of lysophosphatidylcholine (LYPC) (Table 1). Detailed fatty acid analysis in BEL-treated cells revealed that, with time, the proportion of PCs containing polyunsaturated fatty acids, particularly of the n6 group, was significantly

increased, whereas the proportion of PCs with saturated fatty acids decreased and that of monounsaturated fatty acids remained unchanged (Fig. 5A). The ratio of polyunsaturated to saturated hydrocarbon chains in PCs increases significantly in response to treatment with BEL (Fig. 5B). It is possible that this change in ratio profoundly affects the fluidity of the cell membrane (Singer, 1975).

Since n6-containing PCs increased dramatically, we further analyzed this group and found that, in BEL-treated cells, all n6-containing PCs were increased significantly between 8 and 24 hours (Fig. 5C). Our data indicate that the time course of phosphorylation of p53 at Ser15 induced by inhibition of $iPLA_2$ correlates with increasing levels of PCs that contain polyunsaturated fatty acids. Thus, our findings strongly suggest that $iPLA_2$ controls membrane phospholipid homeostasis by regulating levels of polyunsaturated fatty acids in PCs.

PCs with polyunsaturated fatty acids (n6) induce the phosphorylation of p53 at Ser15 through ATR

Since our lipid-profile study in HCT116 cells indicated that inhibition of $iPLA_2$ by BEL causes accumulation of PCs containing polyunsaturated fatty acids, particularly n6-containing PCs, we investigated whether this group of PCs can induce phosphorylation of p53 at Ser15. HCT116 cells were treated with increasing concentrations of PC (18:2n6) for different durations and examined p53-*P* levels by western blot.

As shown in Fig. 6A, PC (18:2n6) induces detectable phosphorylation of p53 at Ser15 after 4 hours. Similar to treatment with BEL (Fig. 1), treatment of cells with PC for 8 hours induced a significant amount of p53-*P* and caused the accumulation of total p53 protein. We also found that PCs that contain a mix of fatty acids (i.e. 15% polyunsaturated fatty acids) induced phosphorylation of p53 at Ser15 in a concentration-dependent manner in U2OS cells (GW33 cells) (Fig. 6B). By contrast, PCs with either monounsaturated (18:1) or saturated fatty acids (16:0) had no apparent effect on phosphorylation of p53 (Fig. 6C).

To determine whether ATR is required for the PC-induced phosphorylation of p53 at Ser15, we analysed the effect of knocking down ATR activity in GK41 cells. GK41 cells were induced with doxycycline and treated with PC(18:2,n6) or PC(18:2,n6) and BEL together. Cells not treated with doxycycline were used as controls. As shown in Fig. 6D, PC(18:2,n6) induced significant phosphorylation of p53 that was further enhanced by BEL alone (without doxycycline). However, in cells expressing ATR-kd the levels of p53-*P* induced by doxycycline were less than those seen in cells without doxycycline induction, demonstrating that ATR is required for the PC(18:2,n6)-induced phosphorylation of p53 at Ser15. Furthermore, we were able to increase both the concentration of the PCs(18:2n6) and the incubation time without inducing DNA damage (Fig. 6E). Taken together, we conclude that $iPLA_2$ regulates the levels of PCs containing polyunsaturated fatty acids in cell membranes. Disruption of this regulation, either by inhibiting $iPLA_2$ or increasing the proportion of PCs that contain polyunsaturated fatty acids, activates ATR and induces the phosphorylation of p53 at Ser15.

Discussion

We report here that inhibition of $iPLA_2$ results in the ATR-dependent phosphorylation of p53 at Ser15 and the increase in the ratio of PCs containing polyunsaturated vs saturated hydrocarbon chains. We further demonstrate that a specific group of PCs (18:2n6) containing polyunsaturated fatty acids can induce the ATR-dependent phosphorylation of p53 at Ser15. Our findings reveal that $iPLA_2$ might play a key role in regulating the levels of polyunsaturated fatty acids in phospholipids. Interestingly, it has been reported that PCs

with linoleic acid in their sn-2 position (18:2n6) serve as a donors for the enrichment of linoleic acid in cardiolipin (Xu et al., 2003), and that $iPLA_2$ hydrolyzes unsaturated fatty acids in PCs at a greater rate than saturated fatty acids (Tang et al., 1997). These findings suggest that, under physiological conditions, cells bulk-synthesize PCs that contain polyunsaturated fatty acids. Subsequently, a negative control mechanism, possibly mediated by $iPLA_2$, is used to precisely regulate their levels in membrane phospholipids.

The fluidity of the lipid bilayers that make up the cell membrane is crucial to their function (Alberts et al., 2002; Singer, 1975; Singer and Nicolson, 1972). It is known that this fluidity is determined mainly by lipid composition and temperature (Alberts et al., 2002; Cevc, 1991; Los and Murata, 2004). Because polyunsaturated fatty acids have low melting points, an increase in the proportion of polyunsaturated fatty acids in phospholipids lowers the melting temperature of a membrane and increases its fluidity (Stubbs and Smith, 1984). The dependence of membrane fluidity on the proportion of polyunsaturated fatty acids has been well demonstrated in organisms whose temperatures fluctuate with their environment (Los and Murata, 2004). For example, the exposure of carp to cold induces the activity of hepatic Δ^9-desaturase, which increases the proportion of polyunsaturated fatty acids in their membranes to maintain a relatively constant fluidity (Tiku et al., 1996).

In mammals, polyunsaturated fatty acids, such as linoleic acid (18:2n6), are the basic constituents of phospholipid membranes. They determine cellular membrane fluidity, and modulate the activities of enzymes, carriers and membrane receptors (Stubbs and Smith, 1984; Zamaria, 2004). Many studies have demonstrated that modification of the polyunsaturated fatty acid composition of mammalian membranes alters their fluidity and function (Stubbs and Smith, 1984; Zamaria, 2004). Interestingly, the membranes of erythrocytes from both mice and humans with Chediak-Higashi Syndrome (CHS) are abnormally fluid (Haak et al., 1979; Ingraham et al., 1981). The proportions of PCs(18:2) in these membranes are also elevated to levels comparable with those seen when $iPLA_2$ is inhibited. Our finding that $iPLA_2$ regulates the ratio of saturated to unsaturated hydrocarbon chains in phospholipids strongly suggests that $iPLA_2$ plays an important role in the regulation of the fluidity of mammalian cellular membranes.

We demonstrate here that ATR, but not ATM, is required for the phosphorylation of p53 at Ser15 in response to increasing ratios of polyunsaturated to saturated hydrocarbon chains in PCs. ATM and ATR, both members of the phosophoinositide 3-kinase related kinase family, directly phosphorylate p53 at Ser15 in response to various types of DNA damage (Canman et al., 1998; Tibbetts et al., 1999). ATM is primarily activated by dsDNA breaks caused by extrinsic agents, such as ionizing radiation and chemotherapeutic drugs (Shiloh, 2006). Since we did not detect any dsDNA or ssDNA damage in response to BEL or PC treatment, it is not surprising that ATM is not involved in the phosphorylation of p53 at Ser15 in response to inhibition of $iPLA_2$.

By contrast, ATR is activated mainly by replication stress, such as ultraviolet-light-induced DNA damage, replication inhibition by aphidicolin or hydroxyurea (Andreassen et al., 2006; Shechter et al., 2004b), or hypoxia in the absence of DNA damage (Hammond and Giaccia, 2004). More importantly, ATR is also essential for normal cell cycle progression: null mutations in mice are embryonic lethal and cells generated from these mice are not viable (Brown and Baltimore, 2000; de Klein et al., 2000) and a splicing mutation affecting expression of ATR is associated with Seckel syndrome in humans (O'Driscoll et al., 2003). In human cells, ATR exists in a stable complex with the ATR-interacting protein (ATRIP) and is activated by ssDNA coated with RPA (replication protein A) (Zou and Elledge, 2003; Zou et al., 2003). It has been shown that ATR is required for fragile-site stability (Casper et al., 2002), the prevention of premature chromatin condensation (Nghiem et al., 2001), and

the regulation of origin firing in response to ssDNA intermediates (Shechter et al., 2004a; Shechter et al., 2004b). Our findings suggest a new role for ATR – one that senses changes in the ratio of polyunsaturated to saturated hydrocarbon chains in phospholipids under physiological conditions.

The nuclear membrane defines the nucleus as the fundamental site of DNA replication. It also controls nucleocytoplasmic exchanges (Nigg, 1997), determines the time of initiation (Leno and Laskey, 1991), and couples DNA replication to the cell cycle (Blow and Laskey, 1988; Leno et al., 1992). PCs in the nuclear membrane of liver contain the highest levels of polyunsaturated fatty acids among phospholipid species (Khandwala and Kasper, 1971), suggesting the importance of PCs that contain polyunsaturated fatty acids in the function of the nuclear membrane. The fact that $iPLA_2$ is localized to the perinuclear region in the presence of glucose and elevated cAMP levels (Ma et al., 2001; Ma et al., 2002) suggests that $iPLA_2$ directly regulates the levels of PCs that contain polyunsaturated fatty acids in order to control the fluidity of the nuclear membrane.

Changes in fluidity can profoundly affect the function of nuclear membranes and the timing of DNA replication. For example, changing the membrane fluidity of vascular smooth muscle cells alters their DNA synthesis (Sachinidis et al., 1999). Since ATR slows the rate of DNA replication in response to transiently generated ssDNA at previously initiated replicons (Shechter et al., 2004b), it will be interesting to determine whether changes in the ratio of polyunsaturated to saturated hydrocarbon chains in phospholipids, especially those in the nuclear membrane, also affect the origin firing of DNA replication. We propose that G1 phospholipid turnover is a programmed event that allows $iPLA_2$ to regulate the fatty acid composition of phospholipids (Fig. 7). Inhibition of $iPLA_2$ causes an increase in the ratio of polyunsaturated to saturated hydrocarbon chains in PCs and might profoundly alter the fluidity and function of the nuclear envelope. In response, the ATR-p53-p21 signalling pathway is activated to prevent cells from inappropriately entering the S phase of the cell cycle.

Materials and Methods

Cell culture and treatment

A rat pancreatic insulin-secreting β-cell line (INS-1), and human carcinoma HCT116 wild type and isogenic HCT116-$p21^{-/-}$ cells were cultured as described elsewhere (Bunz et al., 1998; Seleznev et al., 2006; Song et al., 2005; Zhang et al., 2006). Primary human foreskin fibroblasts (BJ PD27, ATCC no. CRL-2522™) was obtained from ATCC (Manassas, VA) and cultured in MEM medium with 10% fetal bovine serum (FBS). Human B-lymphocyte wild type ($ATM^{+/+}$, GM01805 cells) and ATM-deficient ($ATM^{-/-}$, GM01526 cells) cells were obtained from Coriell Institute for Medical Research (Camden, NJ) and cultured in RPMI medium with 15% heat-inactivated FBS and 2 mM L-glutamine. U2OS-derived osteosarcoma cells with doxycycline-inducible expression of either wild type (ATR-wt, U2OS GW33 cells) or dominant-negative forms of ATR (ATR-kd, U2OS GK41 cells), both gifts from Paul Nghiem, were established and cultured as described (Nghiem et al., 2001; Nghiem et al., 2002). For the induction of ATR-wt in U2OS GW33 cells and ATR-kd in U2OS GK41cells, doxycycline (D9891, Sigma, St Louis, MO) was added to the medium (1 μg/ml) for 2-4 days before harvesting.

For bromoenol lactone (BEL) treatment, the desired numbers of cells were seeded on plates and variable concentrations of freshly prepared BEL (stock at −80°C; Cayman Chemical Co., Ann Arbor, MI) were added and refreshed every 12 hours as necessary (Zhang et al., 2006). For caffeine treatment, caffeine (Sigma) was dissolved in culture medium at stock concentration of 50 mM and applied to cell cultures at a final concentration of 1-5 mM. For

phosphatidylcholine (PC) treatment, four types of PC (Sigma) with variable lengths of polysaturated fatty acids and different numbers of double bonds were used: L-α-PC (P3556), with a fatty acid contents of ~33% 16:0 (palmitic), 13% 18:0 (stearic), 31% 18:1 (oleic), and 15% 18:2 (linoleic acid); PC 18:1 (P3017; 2-oleoyl-1-palmitoyl-sn-glycero-3 phosphocholine); PC 18:2 (P9648; 2-linoleoyl-1-palmitoyl-sn-glycero-3-phosphocholine); and PC 16:0 (P4329; 1,2-dipalmitoyl-*sn*-glycero-3-phosphocholine). Cells were treated with designated concentrations of PCs or with vehicle (100% ethanol) for different periods of time before harvesting.

siRNA silencing of iPLA$_2$ expression

A siRNA pool (SMARTpool siRNA) specifically targeting human iPLA$_2$ was designed and made by Dharmacon (Part of Thermo Fisher Scientific). The siRNA pool contains the following four sense-strand sequences: 5′-AGAUGGAUGUCACCGACUAUU-3′, 5′-CCGCUUCUACUGUGCCAUAUU-3′, 5′-GAGCCUCGUUUCAACCAGAUU-3′ and 5′-GGACGGACAUCAUGCUGGAUU-3′. The control scramble siRNA was also obtained from Dharmacon. The tranfection reagent DharmaFECT was used to deliver siRNA into cells as described by the manufacturer. The amount of siRNA was titrated down from 200 nM; the optimal concentration of siRNA for silencing of iPLA$_2$ was 100 nM. Each sample was analyzed by western blotting 48 hours after transfection.

Western blot analyses

Total cell extracts were prepared in RIPA lysis buffer (United States Biological Inc., Swampscott, MA) with one cocktail of protease inhibitors (Roche) and two phosphatase inhibitors (Sigma, P5726 and P2850). Protein concentrations were determined using the DC protein assay kit (Bio-RAD) and equal amounts of protein (20-50 μg) per lane were subjected to SDS-PAGE electrophoresis. Western blot analyses were performed as described previously (Song et al., 2005; Zhang et al., 2006) using antibodies against iPLA$_2$ (T-14), p53 (C-19), p27 (C-19), MDM2 (C-19), PCNA (C-20) and actin (C-19) (Santa Cruz Biotechnology); p21 (556430) (BD Biosciences); human p53 and p53 phosphorylated at Ser15 (Cell Signalling), and the FLAG tag M5 (F4042) (Sigma).

Immunofluorescence staining and microscopy

Control and treated cells were grown on coverslips for the desired periods of time. Cells were then washed and fixed with a 2% (v/v) formaldehyde solution in PBS for 10 minutes, permeabilized with 0.25% (v/v) Triton X-100 plus 1% NGS for 1 minute and blocked with 0.5% BSA or 1% normal goat serum (NGS) or 1% normal donkey serum (Chemicon International) for 1 hour. For H2AX Ser139 staining, antibody against H2AX phosphorylated at Ser139 (Cell Signalling) was applied and detected using Alexa-Fluor-594-conjugated donkey anti-rabbit IgG (red) (Molecular Probes). For TUNEL analysis, the Apo-BrdU™ Tunel assay kit (Invitrogen Corporation) was used according to the manufacturer's instructions. Alexa-Fluo-488-conjugated donkey anti-goat IgG was used for detection of TUNEL (green).

Stained cells were washed and mounted with the mounting medium Vectashield (Vector Laboratories). The cells were counterstained with 4-6-diamidino-2-phenylindole (DAPI) (blue) and analyzed by fluorescence microscopy with a confocal scanning microscope (Zeiss LSM 510 META) with a ×40, ×63 or ×100 objective. Confocal laser scanning microscopy was performed at the MSSM-Microscopy Shared Resource Facility.

Comet assay for detection of DNA damage

A single-cell gel electrophoresis assay kit, Trevigen's CometAssay, from Trevigen, Inc. was used to detect DNA damage (cat. no. 4250-050-K). The alkaline version of the comet assay was selected because of its ability to measure different types of DNA damage, including single-strand breaks, double-strand breaks, alkali sites (primarily apurinic and apyrimiding sites), incomplete excision repair and DNA crosslinks. Cell samples were prepared immediately before starting the assay, which was performed following the manufacturer's protocol. Briefly, cells were treated with the indicated reagents and harvested. 1×10^5 cells per ml were combined with Comet LMAgarose (Trevigen) at a ratio of 1:10 (v/v) and immediately pipetted onto CometSlide™. The slides were placed at 4°C in the dark to gel and then immersed in freshly prepared alkaline solution (pH>13) for 20-60 minutes in the dark. Slides were then analyzed by electrophoresis, samples air-dried, stained with SYBR Green I and visualized using fluorescence microscopy. The results obtained by this process were quantitatively analyzed using CometScore™ software (AutoComet.com). Multiple metrics were generated to score each comet, including tail length, tail area, % of DNA in the tail, and tail moment. The tail moments (TM=% DNA in tail multiplied by tail length) from multiple cells (all cells on slides) were statistically analyzed.

Phospholipid-profile analysis

Phospholipid profiles were analyzed with TrueMass by Lipomics Technologies Inc. (West Sacramento, CA). Cells were treated with 10 μM BEL or vehicle (control) and samples were prepared at designed time following the manufacturer's instructions. 2.5×10^7 cells of each sample were subjected to phospholipids-profile analysis by TrueMass.

Statistical analysis

Data are expressed as the mean ± s.d. The statistical significance of differences was analyzed using Student's *t*-test, where $P<0.05$ was considered significant.

Supplementary Material

Refer to Web version on PubMed Central for supplementary material.

Acknowledgments

We thank Bert Vogelstein and Kenneth W. Kinzler (Oncology Center, Johns Hopkins University School of Medicine, Baltimore, MA) for providing HCT116-$p53^{+/+}$, $p53^{-/-}$ and $p21^{-/-}$ cell lines; and Paul Nghiem (Division of Dermatology University of Washington Medical Center, Seattle, WA) for providing U2OS GW33 cells (doxycycline-inducible expression of a wild type, ATR-wt) and U20S GK41 cells (doxycycline-inducible expression of a dominant-negative form of ATR, ATR-kd). This work is supported by grants from the National Institutes of Diabetes and Digestive and Kidney Diseases (NIDDK, R01DK063076) and the American Diabetes Association (7-06-RA-87).

References

Alberts, B.; Johnson, A.; Lewis, J.; Raff, M.; Roberts, K.; Walter, P. Molecular Biology of The Cell. Garland Science; New York, NY: 2002.

Andreassen PR, Ho GP, D'Andrea AD. DNA damage responses and their many interactions with the replication fork. Carcinogenesis 2006;27:883–892. [PubMed: 16490739]

Baburina I, Jackowski S. Cellular responses to excess phospholipid. J. Biol. Chem 1999;274:9400–9408. [PubMed: 10092620]

Banin S, Moyal L, Shieh S, Taya Y, Anderson CW, Chessa L, Smorodinsky NI, Prives C, Reiss Y, Shiloh Y, et al. Enhanced phosphorylation of p53 by ATM in response to DNA damage. Science 1998;281:1674–1677. [PubMed: 9733514]

Barak Y, Juven T, Haffner R, Oren M. mdm2 expression is induced by wild type p53 activity. EMBO J 1993;12:461–468. [PubMed: 8440237]

Barbour SE, Kapur A, Deal CL. Regulation of phosphatidylcholine homeostasis by calcium-independent phospholipase A2. Biochim. Biophys. Acta 1999;1439:77–88. [PubMed: 10395967]

Bensaad K, Tsuruta A, Selak MA, Vidal MN, Nakano K, Bartrons R, Gottlieb E, Vousden KH. TIGAR, a p53-inducible regulator of glycolysis and apoptosis. Cell 2006;126:107–120. [PubMed: 16839880]

Blasina A, Price BD, Turenne GA, McGowan CH. Caffeine inhibits the checkpoint kinase ATM. Curr. Biol 1999;9:1135–1138. [PubMed: 10531013]

Blow JJ, Laskey RA. A role for the nuclear envelope in controlling DNA replication within the cell cycle. Nature 1988;332:546–548. [PubMed: 3357511]

Bode AM, Dong Z. Post-translational modification of p53 in tumorigenesis. Nat. Rev. Cancer 2004;4:793–805. [PubMed: 15510160]

Brown EJ, Baltimore D. ATR disruption leads to chromosomal fragmentation and early embryonic lethality. Genes Dev 2000;14:397–402. [PubMed: 10691732]

Bunz F, Dutriaux A, Lengauer C, Waldman T, Zhou S, Brown JP, Sedivy JM, Kinzler KW, Vogelstein B. Requirement for p53 and p21 to sustain G2 arrest after DNA damage. Science 1998;282:1497–1501. [PubMed: 9822382]

Burke B, Ellenberg J. Remodelling the walls of the nucleus. Nat. Rev. Mol. Cell Biol 2002;3:487–497. [PubMed: 12094215]

Campisi J. Senescent cells, tumor suppression, and organismal aging: good citizens, bad neighbors. Cell 2005;120:513–522. [PubMed: 15734683]

Canman CE, Lim D-S, Cimprich KA, Taya Y, Tamai K, Sakaguchi K, Appella E, Kastan MB, Siliciano JD. Activation of the ATM Kinase by Ionizing radiation and phosphorylation of p53. Science 1998;281:1677–1679. [PubMed: 9733515]

Casper AM, Nghiem P, Arlt MF, Glover TW. ATR regulates fragile site stability. Cell 2002;111:779–789. [PubMed: 12526805]

Cevc G. How membrane chain-melting phase-transition temperature is affected by the lipid chain asymmetry and degree of unsaturation: an effective chain-length model. Biochemistry 1991;30:7186–7193. [PubMed: 1854729]

Colanzi A, Suetterlin C, Malhotra V. Cell-cycle-specific Golgi fragmentation: how and why? Curr. Opin. Cell Biol 2003;15:462–467. [PubMed: 12892787]

de Klein A, Muijtjens M, van Os R, Verhoeven Y, Smit B, Carr AM, Lehmann AR, Hoeijmakers JH. Targeted disruption of the cell-cycle checkpoint gene ATR leads to early embryonic lethality in mice. Curr. Biol 2000;10:479–482. [PubMed: 10801416]

Delia D, Mizutani S, Panigone S, Tagliabue E, Fontanella E, Asada M, Yamada T, Taya Y, Prudente S, Saviozzi S, et al. ATM protein and p53-serine 15 phosphorylation in ataxia-telangiectasia (AT) patients and at heterozygotes. Br. J. Cancer 2000;82:1938–1945. [PubMed: 10864201]

Fernandez-Capetillo O, Lee A, Nussenzweig M, Nussenzweig A. H2AX: the histone guardian of the genome. DNA Repair Amst 2004;3:959–967. [PubMed: 15279782]

Gu W, Luo J, Brooks CL, Nikolaev AY, Li M. Dynamics of the p53 acetylation pathway. Novartis Found. Symp 2004;259:197–205. discussion 205-207, 223-225. [PubMed: 15171255]

Haak RA, Ingraham LM, Baehner RL, Boxer LA. Membrane fluidity in human and mouse Chediak-Higashi leukocytes. J. Clin. Invest 1979;64:138–144. [PubMed: 221541]

Hammond EM, Giaccia AJ. The role of ATM and ATR in the cellular response to hypoxia and re-oxygenation. DNA Repair Amst 2004;3:1117–1122. [PubMed: 15279800]

Ingraham LM, Burns CP, Boxer LA, Baehner RL, Haak RA. Fluidity properties and liquid composition of erythrocyte membranes in Chediak-Higashi syndrome. J. Cell Biol 1981;89:510–516. [PubMed: 7251663]

Jackowski S. Coordination of membrane phospholipid synthesis with the cell cycle. J. Biol. Chem 1994;269:3858–3867. [PubMed: 8106431]

Jackowski S. Cell cycle regulation of membrane phospholipid metabolism. J. Biol. Chem 1996;271:20219–20222. [PubMed: 8702749]

Jones RG, Plas DR, Kubek S, Buzzai M, Mu J, Xu Y, Birnbaum MJ, Thompson CB. AMP-activated protein kinase induces a p53-dependent metabolic checkpoint. Mol. Cell 2005;18:283–293. [PubMed: 15866171]

Khandwala AS, Kasper CB. The fatty acid composition of individual phospholipids from rat liver nuclear membrane and nuclei. J. Biol. Chem 1971;246:6242–6246. [PubMed: 4331386]

Kurz EU, Douglas P, Lees-Miller SP. Doxorubicin activates ATM-dependent phosphorylation of multiple downstream targets in part through the generation of reactive oxygen species. J. Biol. Chem 2004;279:53272–53281. [PubMed: 15489221]

Leno GH, Laskey RA. The nuclear membrane determines the timing of DNA replication in Xenopus egg extracts. J. Cell Biol 1991;112:557–566. [PubMed: 1993731]

Leno GH, Downes CS, Laskey RA. The nuclear membrane prevents replication of human G2 nuclei but not G1 nuclei in Xenopus egg extract. Cell 1992;69:151–158. [PubMed: 1555238]

Los DA, Murata N. Membrane fluidity and its roles in the perception of environmental signals. Biochim. Biophys. Acta 2004;1666:142–157. [PubMed: 15519313]

Lykidis A, Jackowski S. Regulation of mammalian cell membrane biosynthesis. Prog. Nucleic Acid Res. Mol. Biol 2001;65:361–393. [PubMed: 11008493]

Ma Z, Turk J. The molecular biology of the group VIA Ca^{2+}-independent phospholipase A2. Prog. Nucleic Acid Res. Mol. Biol 2001;67:1–33. Invited review. [PubMed: 11525380]

Ma Z, Ramanadham S, Wohltmann M, Bohrer A, Hsu FF, Turk J. Studies of insulin secretory responses and of arachidonic acid incorporation into phospholipids of stably transfected insulinoma cells that overexpress group VIA phospholipase A2 (iPLA2beta) indicate a signaling rather than a housekeeping role for iPLA2beta. J. Biol. Chem 2001;276:13198–13208. [PubMed: 11278673]

Ma Z, Zhang S, Turk J, Ramanadham S. Stimulation of insulin secretion and associated nuclear accumulation of iPLA2beta in INS-1 insulinoma cells. Am. J. Physiol. Endocrinol. Metab 2002;282:E820–E833. [PubMed: 11882502]

Massague J. G1 cell-cycle control and cancer. Nature 2004;432:298–306. [PubMed: 15549091]

Matoba S, Kang JG, Patino WD, Wragg A, Boehm M, Gavrilova O, Hurley PJ, Bunz F, Hwang PM. p53 regulates mitochondrial respiration. Science 2006;312:1650–1653. [PubMed: 16728594]

Nghiem P, Park PK, Kim Y.-s. Vaziri C, Schreiber SL. ATR inhibition selectively sensitizes G1 checkpoint-deficient cells to lethal premature chromatin condensation. Proc. Natl. Acad. Sci. USA 2001;98:9092–9097. [PubMed: 11481475]

Nghiem P, Park PK, Kim Y.-s. Desai BN, Schreiber SL. ATR is not required for p53 activation but synergizes with p53 in the replication checkpoint. J. Biol. Chem 2002;277:4428–4434. [PubMed: 11711532]

Nigg EA. Nucleocytoplasmic transport: signals, mechanisms and regulation. Nature 1997;386:779–787. [PubMed: 9126736]

O'Driscoll M, Ruiz-Perez VL, Woods CG, Jeggo PA, Goodship JA. A splicing mutation affecting expression of ataxia-telangiectasia and Rad3-related protein (ATR) results in Seckel syndrome. Nat. Genet 2003;33:497–501. [PubMed: 12640452]

Olive PL, Banath JP. The comet assay: a method to measure DNA damage in individual cells. Nat. Protoc 2006;1:23–29. [PubMed: 17406208]

Rogakou EP, Pilch DR, Orr AH, Ivanova VS, Bonner WM. DNA double-stranded breaks induce histone H2AX phosphorylation on serine 139. J. Biol. Chem 1998;273:5858–5868. [PubMed: 9488723]

Rogakou EP, Nieves-Neira W, Boon C, Pommier Y, Bonner WM. Initiation of DNA fragmentation during apoptosis induces phosphorylation of H2AX histone at serine 139. J. Biol. Chem 2000;275:9390–9395. [PubMed: 10734083]

Sachinidis A, Carniel M, Seewald S, Seul C, Gouni-Berthold I, Ko Y, Vetter H. Lipid-induced changes in vascular smooth muscle cell membrane fluidity are associated with DNA synthesis. Cell Prolif 1999;32:101–105. [PubMed: 10535356]

Sarkaria JN, Busby EC, Tibbetts RS, Roos P, Taya Y, Karnitz LM, Abraham RT. Inhibition of ATM and ATR kinase activities by the radiosensitizing agent, caffeine. Cancer Res 1999;59:4375–4382. [PubMed: 10485486]

Seleznev K, Zhao C, Zhang XH, Song K, Ma ZA. Calcium-independent phospholipase A2 localizes in and protects mitochondria during apoptotic induction by staurosporine. J. Biol. Chem 2006;281:22275–22288. [PubMed: 16728389]

Shechter D, Costanzo V, Gautier J. ATR and ATM regulate the timing of DNA replication origin firing. Nat. Cell Biol 2004a;6:648–655. [PubMed: 15220931]

Shechter D, Costanzo V, Gautier J. Regulation of DNA replication by ATR: signaling in response to DNA intermediates. DNA Repair 2004b;3:901–908. [PubMed: 15279775]

Shiloh Y. The ATM-mediated DNA-damage response: taking shape. Trends Biochem. Sci 2006;31:402–410. [PubMed: 16774833]

Singer SJ. Membrane fluidity and cellular functions. Adv. Exp. Med. Biol 1975;62:181–192. [PubMed: 1106132]

Singer SJ, Nicolson GL. The fluid mosaic model of the structure of cell membranes. Science 1972;175:720–731. [PubMed: 4333397]

Song K, Zhang X, Zhao C, Ang NT, Ma ZA. Inhibition of Ca2+-independent phospholipase A2 results in insufficient insulin secretion and impaired glucose tolerance. Mol. Endocrinol 2005;19:504–515. [PubMed: 15471944]

Stubbs CD, Smith AD. The modification of mammalian membrane polyunsaturated fatty acid composition in relation to membrane fluidity and function. Biochim. Biophys. Acta 1984;779:89–137. [PubMed: 6229284]

Tang J, Kriz RW, Wolfman N, Shaffer M, Seehra J, Jones SS. A novel cytosolic calcium-independent phospholipase A2 contains eight ankyrin motifs. J. Biol. Chem 1997;272:8567–8575. [PubMed: 9079687]

Tibbetts RS, Brumbaugh KM, Williams JM, Sarkaria JN, Cliby WA, Shieh SY, Taya Y, Prives C, Abraham RT. A role for ATR in the DNA damage-induced phosphorylation of p53. Genes Dev 1999;13:152–157. [PubMed: 9925639]

Tiku PE, Gracey AY, Macartney AI, Beynon RJ, Cossins AR. Cold-induced expression of delta 9-desaturase in carp by transcriptional and posttranslational mechanisms. Science 1996;271:815–818. [PubMed: 8629000]

Vogelstein B, Lane D, Levine AJ. Surfing the p53 network. Nature 2000;408:307–310. [PubMed: 11099028]

Xu Y, Kelley RI, Blanck TJ, Schlame M. Remodeling of cardiolipin by phospholipid transacylation. J. Biol. Chem 2003;278:51380–51385. [PubMed: 14551214]

Yang Y, Li CC, Weissman AM. Regulating the p53 system through ubiquitination. Oncogene 2004;23:2096–2106. [PubMed: 15021897]

Zamaria N. Alteration of polyunsaturated fatty acid status and metabolism in health and disease. Reprod. Nutr. Dev 2004;44:273–282. [PubMed: 15460166]

Zhang XH, Zhao C, Seleznev K, Song K, Manfredi JJ, Ma ZA. Disruption of G1-phase phospholipid turnover by inhibition of Ca^{2+}-independent phospholipase A2 induces a p53-dependent cell-cycle arrest in G1 phase. J. Cell Sci 2006;119:1005–1015. [PubMed: 16492706]

Zou L, Elledge SJ. Sensing DNA damage through ATRIP recognition of RPA-ssDNA complexes. Science 2003;300:1542–1548. [PubMed: 12791985]

Zou L, Liu D, Elledge SJ. Replication protein A-mediated recruitment and activation of Rad17 complexes. Proc. Natl. Acad. Sci. USA 2003;100:13827–13832. [PubMed: 14605214]

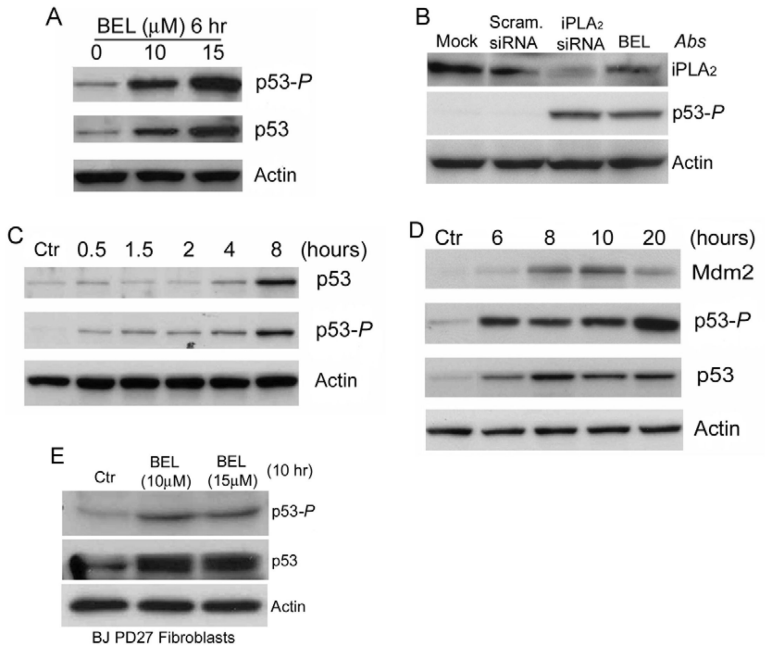

Fig. 1.

Inhibition of $iPLA_2$ induces phosphorylation of p53 at Ser15. (A) Dose-dependent induction of p53 phosphorylation at Ser15 (p53-*P*) by BEL. HCT116 cells were prepared and treated with BEL for 6 hours. The cell lysates were prepared and the levels of p53-*P* and total p53 were determined by western blotting. Actin was used as an internal protein control. (B) siRNA silencing of $iPLA_2$ expression induced phosphorylation of p53. HCT116 cells were transfected with mock, scramble siRNA and siRNA specifically targeting $iPLA_2$. The samples were analyzed by western blotting for $iPLA_2$, p53-*P* and actin. (C) Time course of BEL-induced p53-*P* in HCT116 cells. HCT116 cells were treated with 15 μM BEL for the times indicated. p53-*P* levels were assessed at each time point by western blotting. (D) BEL-induced p53 activation and MDM2 expression. HCT116 cells were incubated with BEL (12.5 μM) or vehicle for up to 20 hours and the levels of p53, p53-*P* and MDM2 were analyzed by western blotting. (E) BEL-induced p53 phosphorylation in primary human foreskin fibroblast BJ PD27 cells. BJ PD27 cells were prepared and treated with BEL for 10 hours. The cell lysates were prepared and the levels of $iPLA_2$, p53-*P* and actin were determined by western blotting.

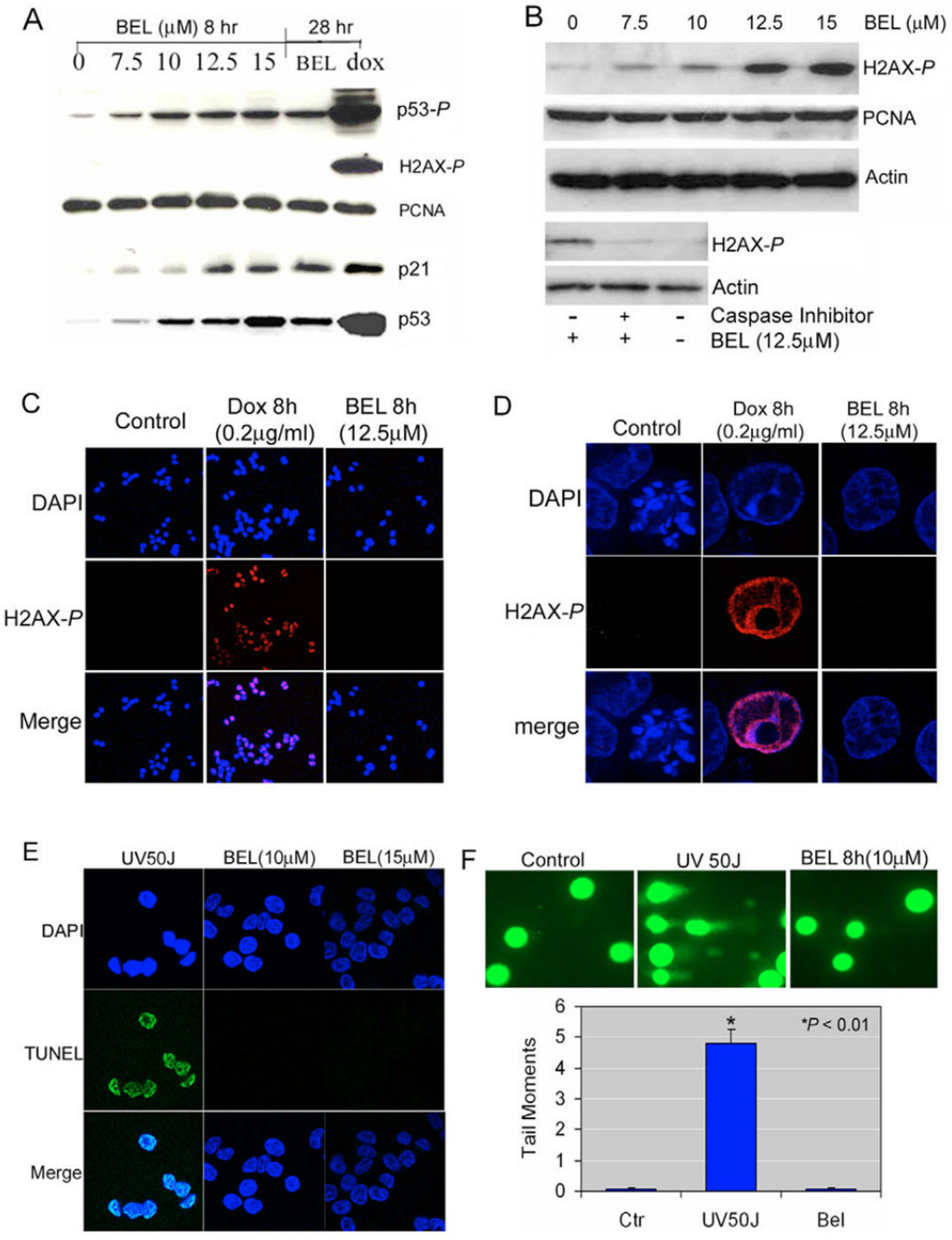

Fig. 2.

Detection of DNA damage by phosphorylation of H2AX at ser 139, TUNEL, and comet assay. (A) Western blot analyses of H2AX-*P*. HCT116 cells were treated with increasing concentration of BEL for 8 or 28 hours. H2AX-*P* and p53-*P*, p21, total p53 and PCNA levels were analyzed by western blotting. Cells treated with doxorubicin (Dox) (1 μg/ml) for 28 hours were used as a positive control for dsDNA breaks. (B) Western blot analysis of H2AX-*P* in HCT116-p21$^{-/-}$ cells. HCT116-p21$^{-/-}$ cells were treated with increasing concentrations of BEL for 8 hours and H2AX-*P* levels were analyzed by western blotting. HCT116-p21$^{-/-}$ cells were next incubated with and without caspase inhibitor (Z-VAD-FMK, 20 μM) for 30 minutes as indicated before being continuously cultured in the

presence or absence of 12.5 μM BEL for 6 hours. H2AX-*P* levels in these cells were analyzed by western blotting. (C) Immunofluorescent staining of H2AX-*P* in multiple HCT116 cells. Cells were treated with vehicle (control), Dox (0.2 μg/ml) for 8 hours, BEL (12.5 μM) for 8 hours. Samples were stained for DAPI (blue) and H2AX-*P* (red) and analyzed by a confocal microscope at ×20 magnification. Merged cells are shown in pink. (D) Immunofluorescent staining of H2AX-*P* in a single nucleus. BEL (12.5 μM, 8 hours) and Dox (0.2 μg/ml, 8 hours) treated cells were stained with anti-H2AX-*P* antibody (red) and DAPI (blue), and individual cells were analyzed using a confocal microscope at ×100 magnification. Merging of H2AX-*P* and DAPI staining in the nucleus appears pink. (E) TUNEL analysis in HCT116 cells. HCT116 cells were treated with 50 J/m^2 UV light and BEL (10 and 15 μM) for 8 hours, and stained using TUNEL (green) and DAPI (blue) followed by the confocal fluorescence microscopy analysis at ×63 magnification. Merging of TUNEL and DAPI staining in the nucleus appear light blue. (F) Comet assay to detect DNA damage in individual cells. HCT116 cells were treated with vehicle (control), 50 J/m^2 of UV light, and 10 μM BEL for 8 hours, respectively. The cells were subjected to an analysis by comet assay. The upper panel showed the results visualized by a fluorescent microscope. The cells with UV light treatment showed the typical ‘comet pattern’ of damaged DNA. The lower panel showed the plot of tail moments (TM) analyzed by the CometScore. More than 50 cells were scored in each condition. There was no significant difference between the BEL treatment and the control. *, significant difference of UV-light treatment from the control or BEL treatment.

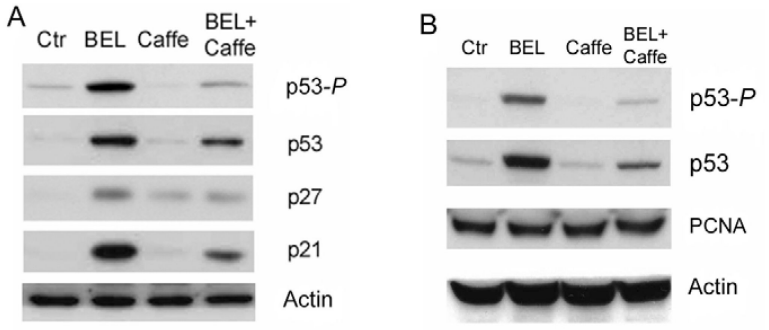

Fig. 3.

BEL-induced phosphorylation of p53 is sensitive to caffeine. (A) BEL-induced phosphorylation in HCT116 cells. HCT116 cells were cultured in the presence and absence of 2.5 mM caffeine for 12 hours and continuously cultured in the presence or absence of 12.5 μM BEL for 12 hours. Cell lysates were analyzed for p53-*P*, p53, p27 and p21 by western blotting. (B) BEL induced p53-*P* and accumulation of p53 in rat pancreatic β-cell line INS-1 cells. INS-1 cells were treated as described in A and cell lysates were analyzed for p53-*P*, p53, PCNA and actin by western blotting.

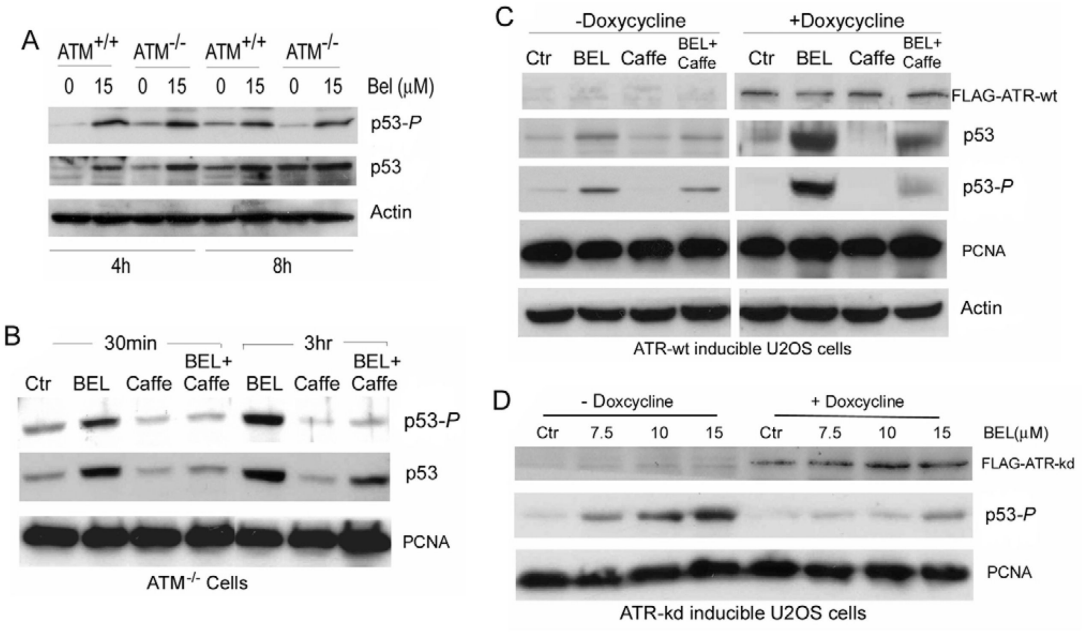

Fig. 4.

BEL induced the phosphorylation of p53 in $ATM^{+/+}$, $ATM^{-/-}$ cells and U2OS cells through doxycycline-stimulated expression of ATR-wt or ATR-kd. (A) Comparison of BEL-induced phosphorylation of p53 in GM01805 ($ATM^{+/+}$) and GM01526 ($ATM^{-/-}$) cells. $ATM^{+/+}$ cells and $ATM^{-/-}$ cells were treated with or without BEL (15 μM) for 4 or 8 hours. Cell lysates were analyzed for p53 and p53-*P* by western blotting. (B) Response to BEL in $ATM^{-/-}$ (GM01526) cells over time. $ATM^{-/-}$ cells were cultured in the absence or presence of caffeine (2.5 mM) for 12 hours and continuously cultured in the presence or absence of BEL (12.5 μM) for 30 minutes and 3 hours. Levels of p53-*P* and p53 were examined by western blotting. (C) BEL-induced phosphorylation of p53-*P* in ATR-wt-inducible U2OS cells. ATR-wt-inducible U2OS cells (GW33) were cultured with or without doxycycline (1 μg/ml) for 1 day. The expression of FLAG-ATR-wt was determined using an anti-FLAG monoclonal antibody. The cells were first cultured in the absence or presence of caffeine (2.5 mM) for 12 hours and then in the absence or presence of BEL (12.5 μM) for 8 hours. Cells were collected and the levels of FLAG-ATR-wt, p53-*P*, p53, PCNA and actin were examined by western blotting. (D) BEL-induced p53-*P* in ATR-kd-inducible U2OS cells. ATR-kd-inducible U2OS cells (GK41) were cultured with or without doxycycline (1 μg/ml) for 1 day. The expression of FLAG-ATR-kd was examined using an anti-FLAG monoclonal antibody. The cells were treated with increasing concentrations of BEL for 8 hours and collected for analysis of FLAG-ATR-kd and p53-*P* by western blotting.

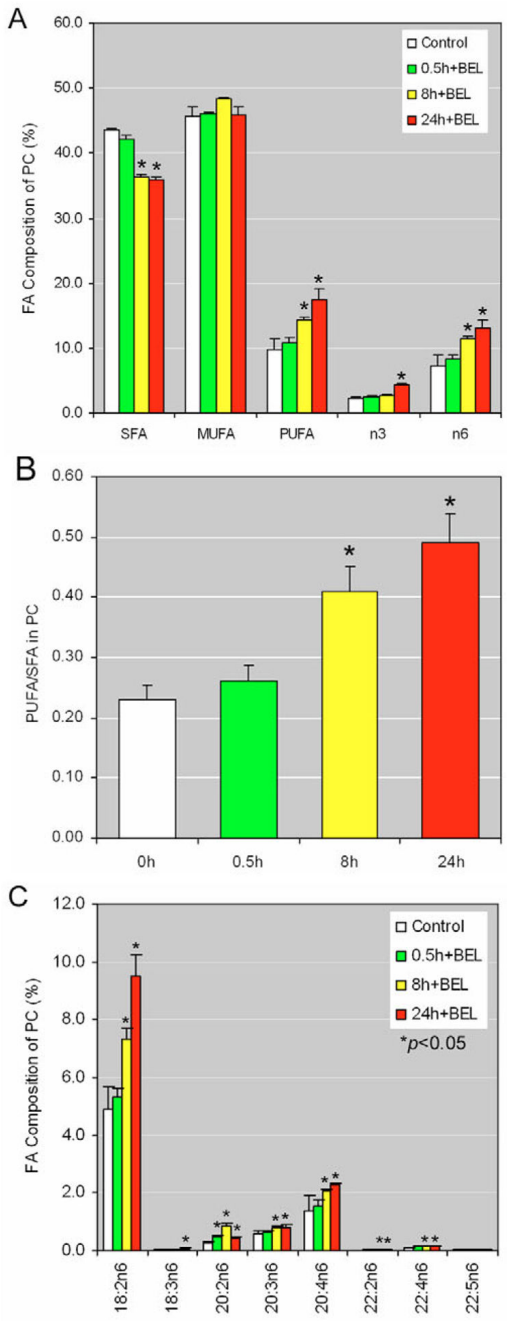

Fig. 5.

Lipid profile of BEL-treated HCT116 cells. (A) HCT116 cells were treated with 10 μM BEL or vehicle (Control) for 0.5, 8 or 24 hours and samples were prepared following the manufacturer's instructions. PC-fatty-acid composition was analyzed by TrueMass. Data represent the results from five repeats.*P<0.05. (B) The ratio of polyunsaturated to saturated fatty acids in PCs of BEL-treated HCT116 cells. Data were calculated using those shown in A. *P<0.05. (C) Cells were prepared as described in A and the composition of those PCs containing 18:2n6-fatty acids was analyzed by TrueMass. *P<0.05.

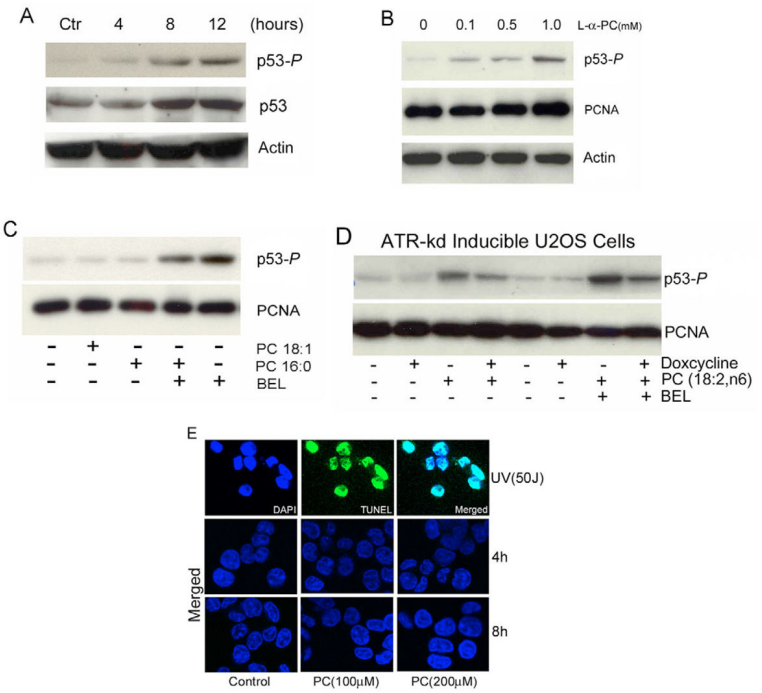

Fig. 6.

PC induces phosphorylation of p53 at Ser15. (A) Time course of PC-induced p53-*P* in HCT116 cells. HCT116 cells were treated with 200 μM of PCs containing polyunsaturated fatty acids (18:2n6), and p53-*P* levels were analyzed at varying time points using western blotting. (B) Dose-dependent induction of p53-*P* by L-α-PC. U2OS (GW33) cells were treated with varying concentrations of L-α-PC for 3 hours and p53-*P* levels were analyzed by western blotting. (C) Effect of PCs containing saturated and monounsaturated fatty acids (8 hours) on p53-*P* in HCT116 cells. (D) PC induction of p53 phosphorylation requires ATR. ATR-kd-inducible U2OS (GK41) cells were induced for expression of ATR-kd with or without doxycycline and then treated with PC alone or a combination of both PC and BEL (7.5 μM) for 8 hours. TUNEL analysis in PC (18:2n6)-treated HCT116 cells. HCT116 cells were treated with 50 J/m^2 UV light, and PCs (100 or 200 μM) for 4 and 8 hours and stained with TUNEL (green) and DAPI (blue) followed by the confocal fluorescence microscopy analysis at ×63 magnification. In merged images of TUNEL and DAPI staining, the nucleus appear light blue. Only the merged images of TUNEL and DAPI staining were shown in the PC-treated cells.

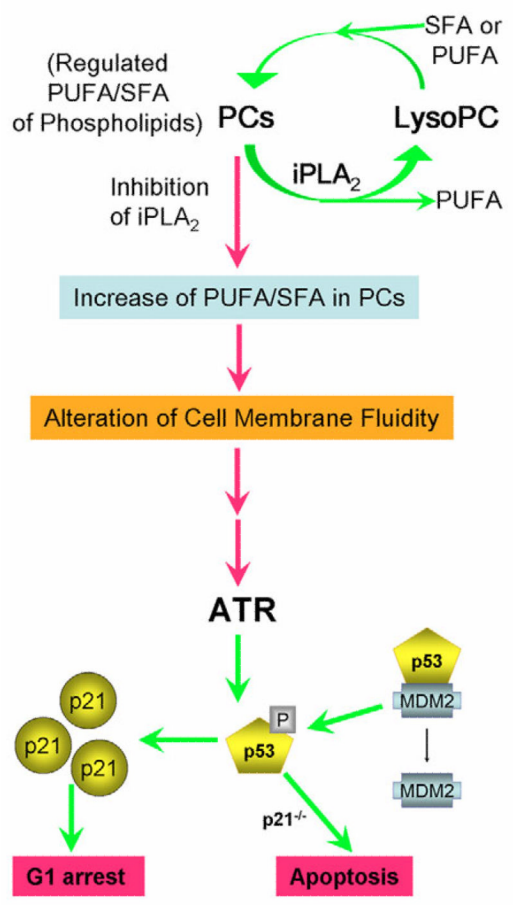

Fig. 7.

Proposed model for activation of the ATR-p53-p21 pathway induced by increasing the amount of PCs that contain polyunsaturated fatty acids in membrane phospholipids. Under physiological conditions, the levels of polyunsaturated fatty acids in cell-membranous PCs in are precisely regulated by a $iPLA_2$-mediated deacylation and reacylation cycle. Inhibition of $iPLA_2$ results in an increase of phospholipids that contain polyunsaturated fatty acids, which may alter the fluidity of cell membranes especially nuclear envelopes. This leads to activation of the ATR-p53-p21 signalling pathway to prevent cells from entering the S phase of the cell cycle. In the absence of p21, the alteration in membrane phospholipids leads to apoptosis (Zhang et al., 2006). PUFA, polyunsaturated fatty acids; SFA, saturated fatty acids; LysoPC, lysophosphatidylcholine.

Table 1

Effect of iPLA2 inhibition on cellular phospholipid profiles

Main classes of phospholipids	Control (% of total)	+BEL (% of total)	*P* value
CL	5.63±0.76	3.12±0.63	<0.10
LYPC	1.68±0.07	1.34±0.15	<0.01
PC	46.54±0.50	48.61±1.42	<0.03
PE	34.89±0.51	34.09±0.65	<0.11
PS	11.26±0.33	11.35±0.29	<0.71

HCT cells were treated with 10 μM BEL (+BEL) or vehicle (control) for 24 hours and samples were prepared following the manufacturer's instructions. Of each sample 2.5×10^7 cells were subjected to phospholipids-profile analysis by TrueMass. Given is the relative amount of each class of phospholipids as the percentage of the total amount of phospholipids. CL, cardiolipin; LYPC, lysophosphatidylcholine; PC, phosphatidylcholine; PE, phosphatidylethanolamine; PS, phosphatidylserine.